



Original Article

Steady State Calculations of the PWR MOX/UO₂ Core with the Monte Carlo Code MCNP6

Nguyen Thi Dung¹, Tran Viet Phu¹, Donny Hartanto²,
Luu Thi Lan³, Mai Huu Thuan⁴, Pham Nhu Viet Ha^{1,*}

¹*Institute for Nuclear Science and Technology, VINATOM, 179 Hoang Quoc Viet, Hanoi, Vietnam*

²*University of Sharjah, P.O.BOX, 27272, Sharjah, United Arab Emirates*

³*Vietnam National Cancer Hospital, 30 Cau Buou, Thanh Tri, Hanoi, Vietnam*

⁴*School of Engineering Physics, HUST, 1 Dai Co Viet, Hai Ba Trung, Hanoi, Vietnam*

Received 13 November 2020

Revised 07 January 2021; Accepted 20 January 2021

Abstract: This paper presents the steady-state analysis results of the OECD/NEA and U.S. NRC PWR MOX/UO₂ (MOX: Mixed Oxide) Core Transient Benchmark with the modern MCNP6 Monte Carlo code based on the ENDF/B-VII.1 evaluated nuclear data library. The purpose of the paper was to verify an MCNP6 model proposed for calculations of a heterogeneous MOX/UO₂ fuelled PWR core, which has different neutronic characteristics from the popular homogeneous ones loaded with the UO₂ fuel due to its partial loading of the MOX fuel. The effective neutron multiplication factors, assembly power distributions, and control rod worths calculated using MCNP6 showed a reasonable agreement within 390 pcm, 6%, and 175 pcm, respectively, with the available benchmark data. The discrepancies between the MCNP6 results and the benchmark data were also discussed. Consequently, the results obtained with MCNP6 and ENDF/B-VII.1 can be considered as a new full-core heterogeneous transport solution to supplement for the available benchmark solutions at the steady-state conditions.

Keywords: PWR, MOX/UO₂, steady state, MCNP6

1. Introduction

It has been recognized that utilizing the recycled plutonium as mixed-oxide (MOX) nuclear fuel in light water reactor cores could save the natural uranium resources and reduce either the amount of

*Corresponding author.

Email address: phamha@vinatom.gov.vn

<https://doi.org/10.25073/2588-1124/vnumap.4621>

weapon-grade plutonium or the plutonium amount which has to be disposed to the final storage. Nevertheless, special concern on the control rod ejection accident (REA), which is a consequence of mechanical failure of the control rod drive mechanism casing located on the reactor pressure vessel top and categorized as design-basis reactivity-initiated accident in pressurized water reactors (PWRs), has also been raised for MOX fueled cores since the neutronics characteristics of plutonium are sufficiently different from uranium [1]. It is noticed that the control rod ejection transient can lead to significant, localized perturbations of the neutronic and thermal-hydraulic core parameters, which can be difficult for reactor core simulators to predict accurately, particularly in a heterogeneous MOX/ UO_2 fueled core. Therefore, partial loading of MOX fuel in a PWR core might call for an improvement of the calculation methods applied in the reactor core simulators. For that reason, the OECD/NEA and U.S. NRC PWR MOX/ UO_2 Core Transient Benchmark [1] has been well defined to provide a framework to assess the heterogeneous transport and nodal diffusion transient methods and codes in predicting the control rod ejection transient response of a PWR MOX/ UO_2 core. However, most of the available benchmark solutions were provided nearly two decades ago and based on the old-fashioned evaluated nuclear data libraries such as ENDF/B-VI. Hence, new benchmark solutions based on modern computer codes and up-to-date evaluated nuclear data libraries are essential to revisit this research topic.

In our ongoing research effort, we aimed at using the 3D reactor kinetics codes PARCS [2] and NODAL3 [3] to revisit the above-mentioned OECD/NEA and U.S. NRC PWR MOX/ UO_2 Core Transient Benchmark. Accordingly, the reactor lattice physics codes including SCALE and Serpent were utilized to prepare the few-group neutron cross-section data for the PWR MOX/ UO_2 transient calculations with PARCS and NODAL3 [4]. In this context, the motivation of the present study was to provide a new full-core heterogeneous transport solution for the benchmark at the steady-state conditions based on the modern MCNP6 Monte Carlo code [5] and the ENDF/B-VII.1 evaluated nuclear data library [6].

Therefore, in this study, the steady-state calculations of the OECD/NEA and U.S. NRC PWR MOX/ UO_2 Core Transient Benchmark were performed using the modern MCNP6 code and the up-to-date ENDF/B-VII.1 library. The goal of the study was to verify an MCNP6 model proposed for calculations of a heterogeneous MOX/ UO_2 fuelled PWR core, which has different neutronic characteristics from the popular homogeneous ones loaded with the UO_2 fuel due to its partial loading of the MOX fuel. The effective neutron multiplication factors, assembly power distributions, and control rod worths were calculated using MCNP6 and compared against the available benchmark data. As a result, these values obtained with MCNP6 and ENDF/B-VII.1 are expected to be a new full-core heterogeneous transport solution for the benchmark at the steady-state conditions.

2. Calculation Model and Method

The one-fourth symmetry of the PWR MOX/ UO_2 core configuration and the main core design parameters are described in Figure 1 and Table 1, respectively. The core has uniform fuel composition in axial direction and the axial reflector has the same width as the fuel assembly pitch. The axial reflector contains fixed moderator at the same conditions with the core inlet and outlet for the bottom and top axial reflectors, respectively. The axial boundary condition (BC) is zero flux. The core is surrounded by a single row of reflector assemblies having the same width as the fuel assembly pitch. Each reflector assembly contains 2.52 cm thick baffle and has fixed moderator at the same conditions with the core inlet. The outer radial BC is zero flux. The PWR UOX (UO_2) and MOX fuel assembly configurations are represented in Figure 2. The UO_2 assembly configuration is a 17×17 lattice including 160 UOX rods, 104 UOX Integral Fuel Burnable Absorber (IFBA) pins and 24 control rods; whereas the MOX assembly

configuration is a 17x17 lattice including 264 MOX rods and 24 Wet Annular Burnable Absorber (WABA) pins. The heavy metal composition in the fuel assemblies is shown in Table 2. Detailed information on the core geometry, the material composition and the benchmark problem can be found in Ref. [1].

In this investigation, the pure 2D problem of the above PWR MOX/ UO_2 core (Part I of the benchmark), with no axial reflector and reflective boundary conditions in the axial direction, at fixed T/H conditions was examined using the Monte Carlo code MCNP6 based on the evaluated nuclear data library ENDF/B-VII.1. The illustration of the PWR MOX/ UO_2 full-core configuration modeled with MCNP6 is provided in Figure 3. The PWR UO_2 and MOX fuel assemblies modelled with MCNP6 are depicted in Figure 4. The reactor conditions that were analysed include HZP (hot zero power) ARO (all rods out) and HZP ARI (all rods in) with the boron concentration of 1,000 ppm. The neutron multiplication factors (eigenvalues), assembly power distributions and control rod worths were calculated using MCNP6 in relation to the available benchmark solutions.

It is worth noting that MCNP6 is a general-purpose Monte Carlo N-Particle transport code developed by the Los Alamos National Laboratory [5] that can be used for neutron, photon, and electron or coupled neutron/photon/electron transport. The MCNP6 code, as an advanced merger of MCNP5 and MCNPX, has various new features, capabilities, and options in addition to those of MCNP5 and MCNPX, allowing its flexibility to be applied in various practical applications such as criticality calculation, reactor design, safety analysis of nuclear facilities, reactor dosimetry. In addition, the ENDF/B-VII.1 evaluated nuclear data library [6] has been extensively validated with the ICSBEP (International Criticality Safety Benchmark Evaluation Project) Benchmark, demonstrating its reliability for criticality calculations [7]. Furthermore, the ENDF/B-VII.1 library was also benchmarked with MCNP6 using the ICSBEP Benchmark, indicating its suitability in combination with MCNP6 particularly for criticality calculations of the low-enriched uranium, compound fuel, thermal spectrum systems (LEU-COMP-THERM) like PWRs [8]. For that reason, the MCNP6 code was selected in the present study along with the ENDF/B-VII.1 library for calculations of the PWR MOX/ UO_2 core.

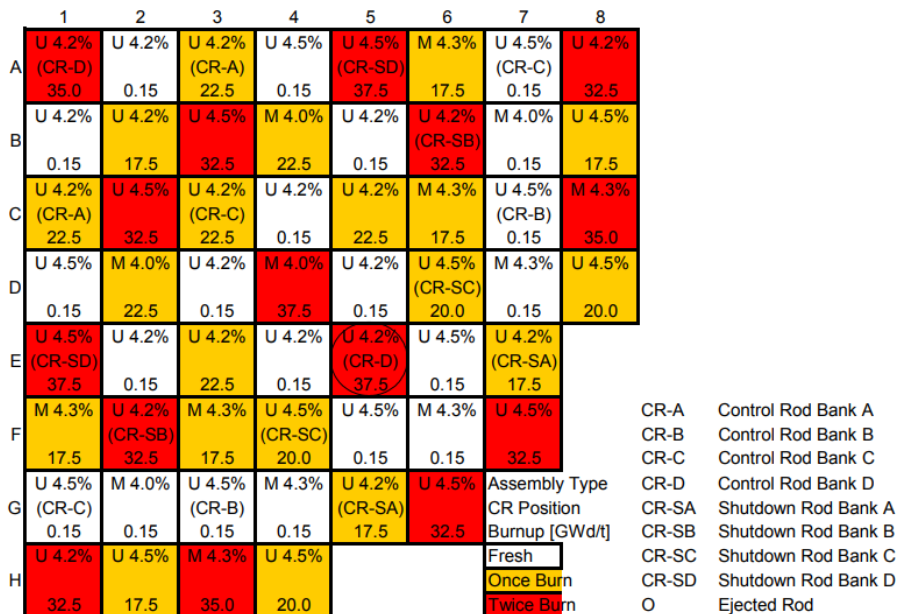


Figure 1. PWR MOX/ UO_2 quarter-core configuration [1].

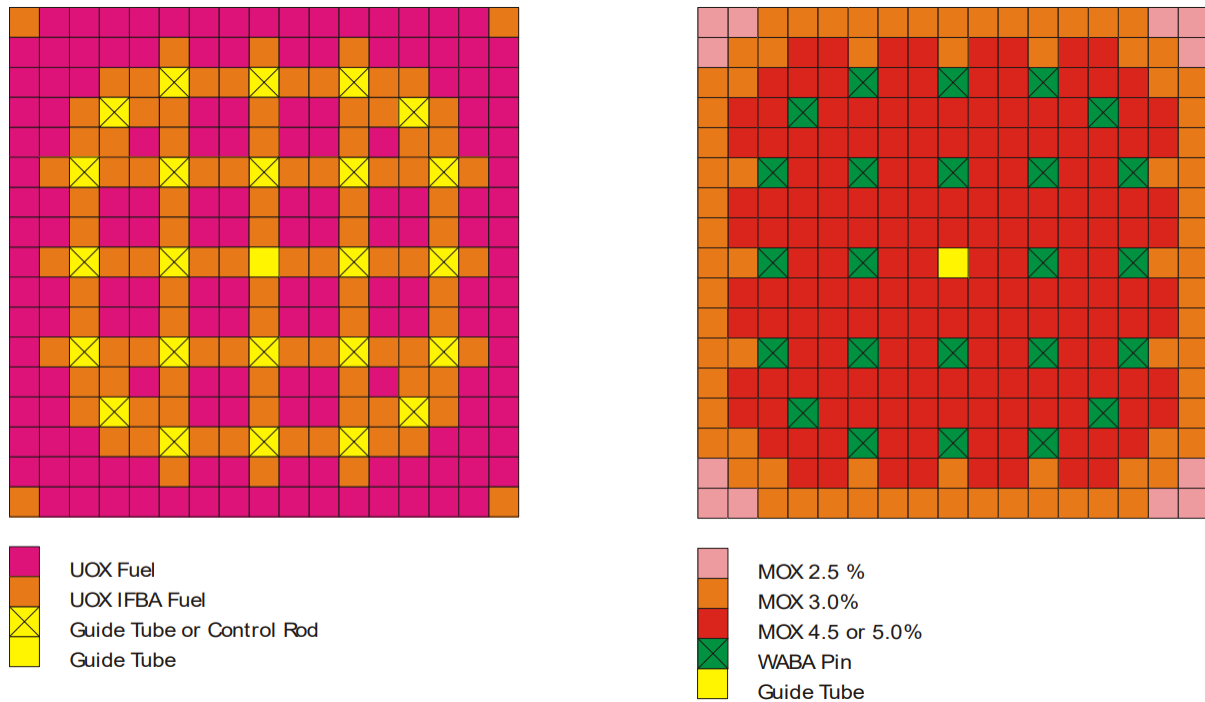
Figure 2. UO₂ (right) and MOX (left) fuel assembly configurations [1].

Table 1. Main core design parameters [1].

Number of fuel assemblies	193
Power level (MWth)	3565
Core inlet pressure (MPa)	15.5
Hot full power (HFP) core average moderator temperature (K)	580.0
Hot zero power (HZP) core average moderator temperature (K)	560.0
Hot full power (HFP) core average fuel temperature (K)	900.0
Fuel lattice, fuel rods per assembly	17x17, 264
Number of control rod guide tubes	24
Number of instrumentation guide tubes	1
Total active core flow (kg/sec)	15849.4
Active fuel length (cm)	365.76
Assembly pitch (cm)	21.42
Pin pitch (cm)	1.26
Baffle thickness (cm)	2.52
Design radial pin-peaking (F_H)	1.528
Design point-wise peaking (F_Q)	2.5
Core loading (tHM)	81.6
Target cycle length (GWd/tHM) (months)	21.564 (18)
Capacity factor (%)	90.0
Target effective full power days	493
Target discharge burnup (GWd/tHM)	40.0-50.0
Maximum pin burnup (GWd/tHM)	62.0
Shutdown margin (SDM) ($\% \Delta\rho$)	1.3

Table 2. Heavy metal (HM) composition in fuel [1].

Assembly type	Density [g/cm ³]	HM material	
UO ₂ 4.2%	10.24	U-235: 4.2 wt%, U-238: 95.8 wt%	
UO ₂ 4.5%	10.24	U-235: 4.5 wt%, U-238: 95.5 wt%	
MOX 4.0%	10.41	Corner zone: 2.5 wt% Pu-fissile	Uranium vector: 234/235/236/238 = 0.002/0.2/0.001/99.797 wt% Plutonium vector: 239/240/241/242 = 93.6/5.9/0.4/0.1 wt%
		Peripheral zone: 3.0 wt% Pu-fissile	
		Central zone: 4.5 wt% Pu-fissile	
MOX 4.3%	10.41	Corner zone: 2.5 wt% Pu-fissile	
		Peripheral zone: 3.0 wt% Pu-fissile	
		Central zone: 5.0 wt% Pu-fissile	

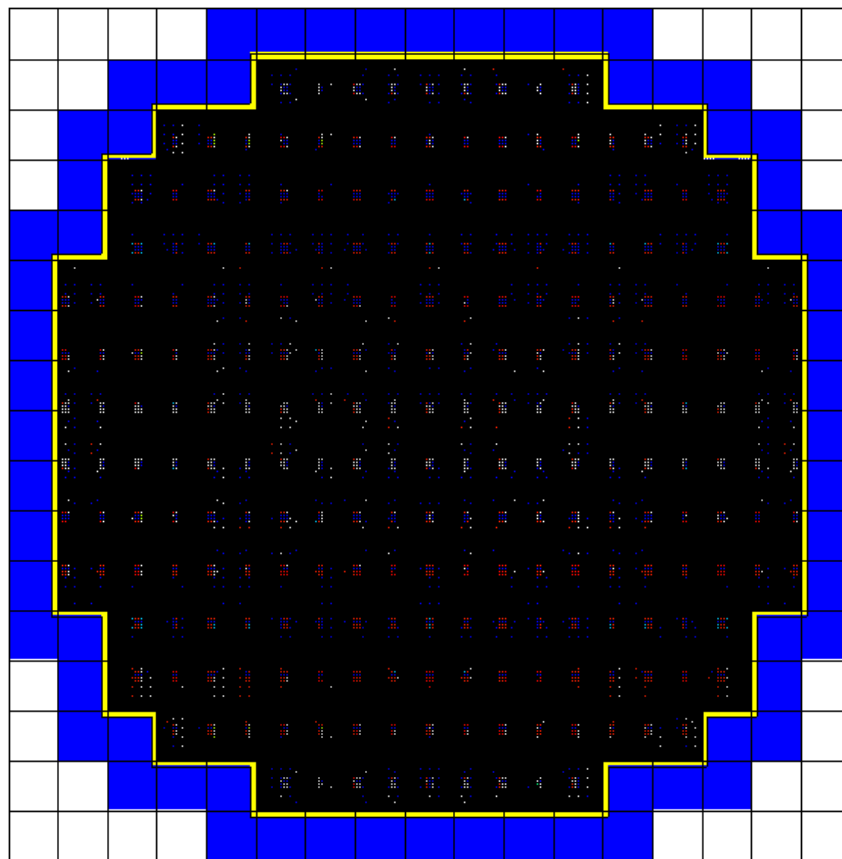


Figure 3. Illustration of the PWR MOX/UO₂ full-core configuration modeled with MCNP6 (inside yellow zone: reactor core; yellow zone: baffle; blue zone: reflector).

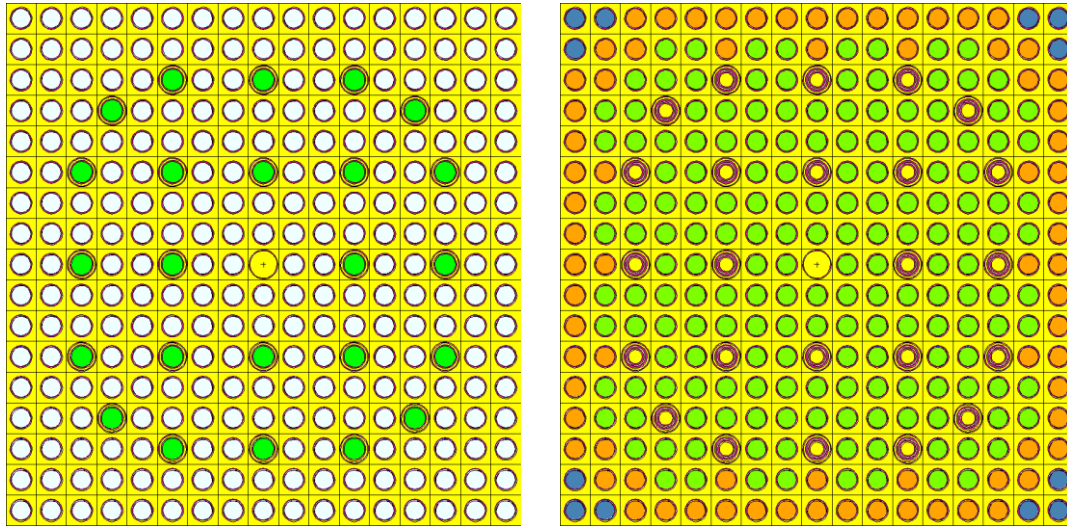


Figure 4. UO_2 (right) and MOX (left) fuel assemblies modeled with MCNP6.

3. Results and Discussion

As given in the benchmark, eight nodal diffusion method based solutions were obtained with the codes CORETRAN, EPISODE, NUREC, PARCS and SKETCH-INS, six of which were two-group (2G) and two were multi-group (MG) [1]. For the heterogeneous transport solutions, two cell homogeneous method based solutions were obtained with the codes BARS and DORT and two full-core heterogeneous method based solutions were obtained with the codes DeCART and MCNP4C2. It is noted that the transport codes without feedback and transient capability, e.g., DORT and MCNP, were able to perform only Part I of the benchmark. Accordingly, the full-core heterogeneous method with the MCNP6 code was applied in this work to solve Part I of the benchmark in comparison with the available benchmark solutions.

The comparison of the assembly power distributions obtained using DeCART and MCNP6 is shown in Figure 5 and Figure 6 at the ARO and ARI conditions, respectively. It can be seen that, at the ARO condition, there was a good agreement within ~4% between DeCART and MCNP6 in predicting the assembly power and the largest discrepancies between the two codes appeared in the high power density regions. Meanwhile, at the ARI condition, the agreement between DeCART and MCNP6 was within ~6% and the largest discrepancies between the two codes appeared in the low power density regions near the fuel assemblies having the control rod banks fully inserted as can be seen in Figure 6.

Table 3 displays the comparison of eigenvalues and assembly power calculated using MCNP6 relative to the benchmark solutions. It can be seen that the MCNP6 results are in good agreement with the benchmark values obtained with different codes at both ARO and ARI conditions. Namely, the difference in the eigenvalues calculated using MCNP6 and the benchmark values was within 390 pcm. Additionally, the total rod worth and the PWE (power-weighted error) and EWE (error-weighted error) values (the definitions of PWE and EWE can be found in Ref. [1]) obtained with MCNP6 were, in general, slightly higher than those obtained with the other codes; e.g., the difference in the predicted total rod worths was within 175 pcm. It might be largely because of the fact that the nuclear data library ENDF/B-VII.1 was used in the MCNP6 calculations as compared to the older ones that were used to obtain the benchmark solutions. In particular, comparing the MCNP6 and MCNP4C2 results as shown

in Table 3 can reveal the discrepancies between using the ENDF/B-VI and ENDF/B-VII.1 libraries; for example, the largest discrepancy in the eigenvalues was 365 pcm while the discrepancy in the total rod worths was 47 pcm.

1.327	1.683	1.395	1.513	1.037	1.051	1.016	0.413
1.667	1.514	1.227	1.281	1.334	0.913	0.995	0.492
1.370	1.208	1.287	1.413	1.237	1.131	1.002	0.398
1.480	1.248	1.414	1.073	1.305	1.143	0.903	0.334
1.026	1.330	1.237	1.306	0.911	1.062	0.577	
1.054	0.927	1.134	1.150	1.073	0.766	0.280	
0.999	1.004	1.005	0.913	0.586	0.281		
0.418	0.495	0.407	0.347				
1.374	1.735	1.418	1.525	1.035	1.032	0.997	0.413
1.735	1.563	1.245	1.277	1.349	0.918	0.978	0.491
1.418	1.245	1.325	1.446	1.247	1.114	0.991	0.393
1.525	1.277	1.446	1.076	1.308	1.143	0.892	0.341
1.035	1.348	1.247	1.308	0.904	1.067	0.585	
1.032	0.917	1.114	1.142	1.067	0.754	0.281	
0.997	0.978	0.991	0.892	0.585	0.281		
0.413	0.491	0.393	0.34				
-3.440	-2.979	-1.652	-0.786	0.206	1.808	1.896	0.105
-3.944	-3.137	-1.455	0.291	-1.147	-0.571	1.766	0.186
-3.400	-2.993	-2.867	-2.296	-0.795	1.530	1.073	1.344
-2.982	-2.258	-2.221	-0.242	-0.199	0.022	1.235	-2.165
-0.872	-1.312	-0.782	-0.118	0.827	-0.510	-1.420	
2.087	1.067	1.811	0.721	0.602	1.601	-0.426	
0.242	2.695	1.382	2.302	0.250	0.082		
1.302	0.809	3.642	2.021				

Figure 5. Assembly power distributions obtained by MCNP6 (this work) (top) and DeCART (middle) and relative difference (%) between MCNP6 and DeCART (bottom) at ARO condition.

1.182	2.484	1.213	2.219	0.764	0.681	0.301	0.207
2.487	2.442	1.830	2.187	1.897	0.466	0.499	0.267
1.224	1.837	1.235	2.556	2.034	1.045	0.342	0.200
2.249	2.193	2.541	1.925	1.758	0.554	0.462	0.179
0.760	1.889	2.022	1.735	0.533	0.708	0.197	
0.666	0.456	1.020	0.554	0.714	0.587	0.193	
0.288	0.478	0.330	0.452	0.195	0.191		
0.193	0.260	0.199	0.181				
1.209	2.533	1.202	2.196	0.742	0.669	0.300	0.205
2.533	2.459	1.812	2.103	1.832	0.449	0.489	0.268
1.202	1.812	1.198	2.452	1.944	0.985	0.329	0.198
2.196	2.103	2.452	1.823	1.675	0.531	0.450	0.186
0.742	1.832	1.944	1.675	0.508	0.696	0.190	
0.669	0.449	0.985	0.531	0.696	0.562	0.186	
0.300	0.489	0.329	0.450	0.190	0.186		
0.205	0.268	0.198	0.186				
-2.242	-1.918	0.903	1.052	2.931	1.803	0.449	1.144
-1.813	-0.682	0.999	4.013	3.542	3.720	2.115	-0.196
1.850	1.379	3.114	4.232	4.605	6.115	3.850	1.058
2.424	4.302	3.618	5.618	4.979	4.421	2.724	-3.595
2.489	3.135	4.024	3.594	4.831	1.750	3.638	
-0.447	1.561	3.557	4.395	2.538	4.391	3.771	
-3.857	-2.258	0.233	0.486	2.397	2.450		
-5.619	-3.014	0.310	-2.434				

Figure 6. Assembly power distributions obtained by MCNP6 (this work) (top) and DeCART (middle) and relative difference (%) between MCNP6 and DeCART (bottom) at ARI condition.

The single rod worths at the ARO and ARI conditions were also calculated using MCNP6 and shown in Tables 4 and 5 in relation to the benchmark solutions, respectively. At the ARO condition, the single rod worths predicted using MCNP6 agree with the benchmark values within 31 pcm. At the ARI condition, the agreement between the MCNP6 and benchmark solutions was found to be within 56 pcm. Moreover, it can be seen that the MCNP results generally overestimated the benchmark solutions at both ARO and ARI conditions. Such discrepancies between the MCNP6 and benchmark solutions might be mainly contributed by (1) the use of the newer nuclear data library ENDF/B-VII.1 in the MCNP6 calculations as compared to the older ones that were used to obtain the benchmark solutions and (2) the difference in the neutron transport solution method that was employed in each code. In addition, those discrepancies between the MCNP6 and benchmark solutions also suggest that a more detailed analysis of single rod worths for a PWR MOX/UO₂ core predicted using Monte Carlo and deterministic methods should be carefully examined in future work.

Table 3. Comparison of eigenvalues and assembly power.

	Eigenvalue		Total rod worth (dk/k)	Assembly power error			
	ARO	ARI		ARO		ARI	
				%PWE	%EWE	%PWE	%EWE
nodal							
CORETRAN 1/FA	1.06387	0.99202	6808	1.06	1.69	2.01	2.52
CORETRAN 4/FA	1.06379	0.99154	6850	0.96	1.64	1.67	2.18
EPISODE	1.06364	0.99142	6849	0.96	1.64	1.66	2.16
NUREC	1.06378	0.99153	6850	0.96	1.63	1.64	2.16
PARCS 2G	1.06379	0.99154	6850	0.96	1.63	1.67	2.18
PARCS 4G	1.06376	0.99136	6865	0.90	1.42	1.61	2.26
PARCS 8G	1.06354	0.99114	6868	0.86	1.25	1.65	2.49
SKETCH-INS	1.06379	0.99153	6850	0.97	1.67	1.67	2.16
heterogeneous							
BARS	1.05826	0.98775	6745	1.29	1.92	3.92	10.30
DeCART	1.05852	0.98743	6801	reference	reference	reference	reference
DORT	1.06036	-	-	0.86	1.12	-	-
MCNP4C2	1.05699	0.98540	6873	0.67	1.26	1.33	3.67
MCNP6 (this work)	1.06064	0.98812	6920	1.59	2.21	2.9	3.59

Table 4. Comparison of single rod worths at ARO condition (dk/k).

	Rod position									
	(A,1)	(A,3)	(A,5)	(A,7)	(B,6)	(C,3)	(C,7)	(D,6)	(E,5)	(E,7)
nodal										
CORETRAN 1/FA	164	143	91	53	70	122	51	68	64	28
CORETRAN 4/FA	166	144	92	53	70	123	51	69	65	28
EPISODE	165	134	-	53	70	123	51	69	64	27
NUREC	166	143	91	53	70	122	51	68	64	27
PARCS 2G	166	143	91	53	70	123	51	68	64	27
PARCS 4G	167	144	91	53	70	122	51	68	64	27
PARCS 8G	168	144	91	52	69	123	50	68	64	27
SKETCH-INS	166	143	91	53	70	123	51	68	64	27

heterogeneous										
BARS	166	139	87	49	66	117	49	66	63	27
DeCART	-	-	-	-	-	-	-	-	-	-
DORT	-	-	-	-	-	-	-	-	-	-
MCNP4C2	-	-	-	-	-	-	-	-	-	-
MCNP6 (this work)	182	154	118	43	86	122	61	94	72	30

Table 5. Comparison of single rod worths at ARI condition (dk/k).

	Rod position									
	(A,1)	(A,3)	(A,5)	(A,7)	(B,6)	(C,3)	(C,7)	(D,6)	(E,5)	(E,7)
nodal										
CORETRAN 1/FA	-826	-875	-397	-57	-151	-1115	-78	-291	-246	-22
CORETRAN 4/FA	-840	-880	-405	-55	-152	-1127	-78	-290	-249	-20
EPISODE	-843	-884	-	-59	-155	-1130	-81	-293	-253	-24
NUREC	-840	-880	-405	-56	-152	-1127	-78	-290	-249	-21
PARCS 2G	-840	-880	-405	-56	-152	-1127	-78	-290	-249	-21
PARCS 4G	-849	-886	-407	-55	-153	-1134	-77	-290	-250	-21
PARCS 8G	-857	-889	-409	-54	-153	-1139	-76	-290	-253	-20
SKETCH-INS	-840	-880	-405	-56	-152	-1127	-78	-290	-249	-21
heterogeneous										
BARS	-914	-921	-417	-44	-145	-1193	-68	-313	-268	-17
DeCART	-	-	-	-	-	-	-	-	-	-
DORT	-	-	-	-	-	-	-	-	-	-
MCNP4C2	-	-	-	-	-	-	-	-	-	-
MCNP6 (this work)	-882	-895	-433	-73	-154	-1142	-97	-312	-285	-48

4. Conclusion

In this work, the steady-state calculations of the OECD/NEA and U.S. NRC PWR MOX/ UO_2 Core Transient Benchmark were performed using the modern MCNP6 Monte Carlo code and the ENDF/B-VII.1 evaluated nuclear data library. The eigenvalues, assembly power distributions, and control rod worths calculated using MCNP6 exhibited a reasonable agreement within 390 pcm, 6%, and 175 pcm, respectively, with the available benchmark solutions. The discrepancy between the MCNP6 and benchmark solutions, especially when comparing the single rod worths, might be largely contributed by (1) the use of the newer nuclear data library ENDF/B-VII.1 in the MCNP6 calculations as compared to the older ones that were used to obtain the benchmark solutions and (2) the difference in the neutron transport solution method that was employed in each code. Consequently, these results obtained with MCNP6 and ENDF/B-VII.1 can be considered as a new full-core heterogeneous transport solution to supplement for the available benchmark solutions at the steady-state conditions. Furthermore, the MCNP6 model and the results obtained herein can be applied to verify our MOX/ UO_2 fuelled PWR core models being developed with the reactor kinetics codes PARCS and NODAL3, which in turn will be used for further analyses of REAs in a MOX/ UO_2 fuelled PWR core. Besides, another potential applicability of the MCNP6 model developed is that it can be easily extended to 3D for neutronics analyses, in particular for fuel depletion calculations, of a PWR MOX/ UO_2 core thanks to various powerful features and capabilities, e.g., the depletion capability of the Monte Carlo MCNP6 code.

Acknowledgments

This research was funded by the National Foundation for Science and Technology Development (NAFOSTED) under Grant 103.99-2018.32.

References

- [1] T. Kozłowski, T. J. Downar, PWR MOX/UO₂ Core Transient Benchmark Final Report, Purdue University, ISBN 92-64-02330-5, NEA/NSC/DOC 20, US, 2006.
- [2] T. J. Downar, Y. Xu, V. Seker, N. Hudson, User Manual for the PARCS v3.0 U.S. NRC Core Neutronics Simulator, University of Michigan, UM-NERS-09-0001, US, 2012.
- [3] S. Pinem, T. M. Sembiring, P. H. Liem, The Verification of Coupled Neutronics Thermal-Hydraulics Code NODAL3 in the PWR Rod Ejection Benchmark, Science and Technology of Nuclear Installations, Vol. 2014, 2014, Article ID 845832, <https://doi.org/10.1155/2014/845832>.
- [4] T. M. Vu, D. Hartanto, T. T. Anh, L. T. Lan, T. V. Phu, P. N. V. Ha, Neutron Cross Section Generation for PWR MOX Fuel Assemblies with SCALE and Serpent, VNU Journal of Science: Mathematics – Physics, Vol. 37, No. 2, 2021, pp. 59-68, <https://doi.org/10.25073/2588-1124/vnumap.4596>.
- [5] D. B. Pelowitz (editor), MCNP6TM User's Manual Version 1.0, Los Alamos National Laboratory, LA-CP-13-00634, Rev. 0, US, 2013.
- [6] M. B. Chadwick, M. Herman, P. Obložinský, M. E. Dunn, Y. Danon, A. C. Kahler, D. L. Smith, B. Pritychenko, G. Arbanas, R. Arcilla, R. Brewer, D. A. Brown, R. Capote, A. D. Carlson, Y. S. Cho, H. Derrien, K. Guber, G. M. Hale, S. Hoblit, S. Holloway, T. D. Johnson, T. Kawano, B. C. Kiedrowski, H. Kim, S. Kunieda, N. M. Larson, L. Leal, J. P. Lestone, R. C. Little, E. A. McCutchan, R. E. MacFarlane, M. MacInnes, C. M. Mattoon, R. D. McKnight, S. F. Mughabghab, G. P. A. Nobre, G. Palmiotti, A. Palumbo, M. T. Pigni, V. G. Pronyaev, R. O. Sayer, A. A. Sonzogni, N. C. Summers, P. Talou, I. J. Thompson, A. Trkov, R. L. Vogt, S. C. van der Marck, A. Wallner, M. C. White, D. Wiarda, P. G. Young, ENDF/B-VII.1 Nuclear Data For Science and Technology: Cross Sections, Covariances, Fission Product Yields and Decay Data, Nuclear Data Sheets, Vol. 112, No. 12, 2011, pp. 2887-2996, <https://doi.org/10.1016/j.nds.2011.11.002>.
- [7] A. C. Kahler, R. E. MacFarlane, R. D. Mosteller, B. C. Kiedrowski, S. C. Frankle, M. B. Chadwick, R. D. McKnight, R. M. Lell, G. Palmiotti, H. Hiruta, M. Herman, R. Arcilla, S. F. Mughabghab, J. C. Sublet, A. Trkov, T. H. Trumbull, M. Dunn, ENDF/B-VII.1 Neutron Cross Section Data Testing With Critical Assembly Benchmarks and Reactor Experiments, Nuclear Data Sheets, Vol. 112, No. 12, 2011, pp. 2997-3036, <https://doi.org/10.1016/j.nds.2011.11.003>.
- [8] S. C. Marck, Benchmarking ENDF/B-VII.1, JENDL-4.0 and JEFF-3.1.1 with MCNP6, Nuclear Data Sheets, Vol. 113, No. 12, 2012, pp. 2935-3005, <https://doi.org/10.1016/j.nds.2012.11.003>.